ISSN 2706-655X Vol.5, Issue 12: 106-110, DOI: 10.25236/IJFET.2023.051216

Damage mechanism and evidence of anchor solid under static and dynamic loading conditions

Mengxiang Ma[1], Yunhai Cheng[*]

[1]Department of Mining Engineering, Anhui University of Science and Technology, Huainan, China
[*]Corresponding author

Abstract: *Aiming at the impact damage problem of anchorage structure under the condition of superimposed dynamic and static loads, based on the solution of Kelvin elasticity problem, an analytical model of anchor force under the joint action of pre-stretching static load and blasting dynamic load is established, and based on the reflecting and transmitting process of the stress wave between the anchorage and free sections of the anchorage, an analytical model of the force of end-anchored anchorage under the joint action of pre-stretching static load and blasting dynamic load is put forward, and the corresponding damage is given. The analytical model is proposed and the corresponding damage form is given. It is found that due to the different wave impedance of the free section, the anchored section and the roadway surface, the axial stresses superimposed on the anchors at different locations are different. Meanwhile, due to the complex nature of the surrounding rock, the differences in anchor rods and anchor materials, and the construction errors, the damage forms of the anchorage bearing structure are different.*

Keywords: *dynamic and static loads, anchor solid, Impact dynamic load*

1. Introduction

With the decrease of shallow coal resources, deep mining becomes the development trend. Unlike shallow roadway anchors, deep roadway anchor support structures are not only subjected to pre-tensioned static loads, but also to dynamic loads such as blasting. In recent decades, the mechanical properties of anchoring systems have been widely studied.

Based on the Kelvin displacement solution, Jianchao Zhang [1] and others analyzed the effect of axial force and shear stress distribution in the anchored section of anchor rods when the hole diameter, the elastic modulus of the surrounding rock and soil, and the tension load on the distribution of the axial force and shear stress in the anchored section by deriving the expression equation for the distribution of the axial force and shear stress in the anchored section of the anchor rods. You Chun'an [2] derived the expression formula of stress and bearing plate distance through theoretical study based on the displacement solution of Mindlin problem. The results of the study show that: under the action of pullout load, the peak of anchor shear stress did not appear at the orifice; in the elastic state the anchor is subjected to a small range of shear stress; the magnitude and distribution of shear stress are related to the nature of the rock mass. Zhao Minghua [3] and others established the energy balance equation based on the energy principle and derived the anchor solid load-displacement calculation equation. Huang Liuyun [4] et al. established the theoretical equations for axial and shear stresses of the anchored segment of the anchor bar in the soil body based on the Kelvin solution. Wang Mingshu [5] et al. proposed the neutral point theory through theoretical and experimental studies, which suggests that a section of anchor rods close to the roadway will prevent the surrounding rock from moving outward, and in a section of anchor rods away from the roadway, the surrounding rock will prevent the anchor rods from moving, so that the anchor rods are subjected to shear force backward to the roadway, and the place where the shear force is zero is the neutral point of the anchor rods. Although the test results of some domestic scholars proved the theory, and the neutral point theory has been generally accepted, but the phenomenon of anchor rod tail fracture is still unexplained. Yang Gengshe [6] and others proposed the neutral point formula of bonded anchors with pallets by studying bonded anchors with pallets, and analyzed that the neutral point is not fixed through the study. Wang Wenjie [7] and others used numerical analysis to show that full-length anchored prestressed FRP anchors can effectively change the position of the neutral point of the anchor compared with threaded steel anchors, improve the stress distribution characteristics of the anchorage, and increase the ability of the anchor and anchorage to resist the deformation of the surrounding rock to

ISSN 2706-655X Vol.5, Issue 12: 106-110, DOI: 10.25236/IJFET.2023.051216

the wall.

However, the above research mainly focuses on the stress distribution and load transfer mechanism of anchor rods under the action of pre-stretch static load, while the research on the mechanical properties of anchor rods under the joint action of pre-stretch static load and blasting dynamic load is relatively small, and most of them are numerical analysis and practical experience, the theory lags behind the practice, which can't satisfy the needs of FRP anchor support design and mining blasting control.

2. Force modeling of end-anchored anchors under pre-tensioned static loads

The anchors are often supported with a certain amount of prestressing applied through the pallet nut at the end, so the FRP anchors will be subjected to both static and dynamic loads together under blasting dynamic loads. The force model of the end-anchored anchor under pre-stretching static load is shown in Fig. 1. The expression of axial stress σ(x) at point x on the anchor can be written as Equation 1.

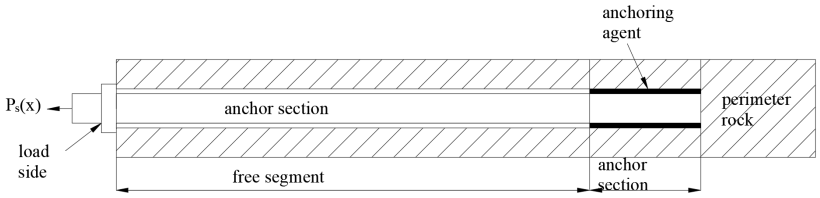

Figure 1: Analytical model of end anchor force during static load pullout

$$\sigma(x)=\begin{cases}\dfrac{E_b a}{b}\dfrac{1}{\left(1+e^{-\frac{L_2-x_0}{b}}\right)}(0\le x\le L_1)\\ \dfrac{E_b a}{b}\dfrac{1}{\left(1+e^{-\frac{L_2-x-x_0}{b}}\right)}(L_1\le x\le L_1+L_2)\end{cases} \tag{1}$$

Where Eb is the modulus of elasticity of the anchor; a, b are constant parameters related to the material properties of the anchor; D is the diameter of the anchor; x0 is the parameter determined by the pullout test.

The coefficient x0 related to the static load force can be calculated by the following equation (2):

$$x_0 = L + bln\left(\frac{a\pi D^2 E_b}{4bP_s}-1\right) \tag{2}$$

Where: Ps is the preload force applied to the anchor bar

3. Force modeling of end-anchored anchors under dynamic loads

As shown in Fig. 2, when the incident compression wave σ_{d0} propagates to the interface 1, the wave impedance $\rho_1 c_1$ is larger than the wave impedance $\rho_2 c_2$, so the reflected wave σ_{r1} is a stretching wave; when the transmitted compression wave σ_{t1} propagates to the interface 2, the transmitted compression wave σ_{t1} is almost completely reflected as a stretching wave σ_{r2} because the wave impedance $\rho_3 c_3$ is 0; when the reflected stretching wave σ_{r2} propagates to the interface 2 again, it will generate reflected stretching wave σ_{r3} and transmitted stretching wave σ_{t2}; the whole process is a cycle of stress wave. When the reflected tensile wave σ_{r2} propagates to the interface 2 again, the reflected tensile wave σ_{r3} and the transmitted tensile wave σ_{t2} will be generated; the whole process is a cyclic cycle of the stress wave.

ISSN 2706-655X Vol.5, Issue 12: 106-110, DOI: 10.25236/IJFET.2023.051216

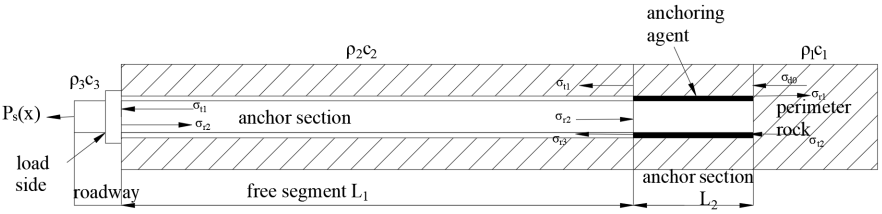

Figure 2: Equivalent schematic of wave impedance

$$\sigma_{d0} = \rho_r c_r v \tag{3}$$

$$v = \frac{e^{3.95+0.57M_l}}{R} \tag{4}$$

By formula

$$\begin{cases} \sigma_t = \frac{2}{n+1}\sigma_{d0} \\ \sigma_r = \frac{1-n}{n+1}\sigma_{d0} \\ n = \sqrt{\frac{\rho_a E_a}{\rho_b E_b}} \end{cases} \tag{5}$$

Where: ρ_a, ρ_b are the density of the medium a, b two sides;

E_a, E_b for the medium a, b two sides of the elastic modulus;

According to Eqs. (3), (4) and (5), the reflected and transmitted stresses at interface 1 and interface 2 can be obtained.

where the reflected and transmitted stresses at interface 1 are:

$$\sigma_{t_1} = \frac{2}{n_1+1}\sigma_d = -\frac{2}{n_1+1}\rho_r c_r \frac{e^{3.95+0.57M_l}}{R} \tag{6}$$

$$\sigma_{r_1} = -\frac{1-n_1}{n_1+1}\sigma_d = \frac{1-n_1}{n_1+1}\rho_r c_r \frac{e^{3.95+0.57M_l}}{R} \tag{7}$$

The reflected stress at interface 2 is:

$$\sigma_{r_2} = -\frac{2}{n_1+1}\sigma_{t_1} = \frac{2}{(n_1+1)}\rho_r c_r \frac{e^{3.95+0.57M_l}}{R} \tag{8}$$

When the stress wave propagates to interface 2 for the second time, the reflected stress and transmission stress at interface 2 are as follows:

$$\sigma_{t2} = \frac{2}{n_3+1}\sigma_{r_2} = \frac{4}{(n_1+1)(n_3+1)}\rho_r c_r \frac{e^{3.95+0.57M_l}}{R} \tag{9}$$

$$\sigma_{r3} = \frac{1-n_3}{n_s+1}\sigma_{r_2} = \frac{2(1-n_s)}{(n_1+1)(n_3+1)}\rho_r c_r \frac{e^{3.95+0.57M_l}}{R} \tag{10}$$

Among them:$\mathrm{n}_1 = \sqrt{\frac{\rho_1 \mathrm{E}_1}{\rho_2 \mathrm{E}_2}}$; $\mathrm{n}_2 = \sqrt{\frac{\rho_2 \mathrm{E}_\mathrm{s}}{\rho_\mathrm{s} \mathrm{E}_\mathrm{s}}}$; $\mathrm{n}_\mathrm{s} = \sqrt{\frac{\rho_2 \mathrm{E}_2}{\rho_1 \mathrm{E}_1}}$

Considering the complexity of plane stress wave propagation in the end anchorage structure and the rapid attenuation of the energy carried by the stress wave, only a single cycle propagation of the blast stress wave is considered in this paper. After the stress wave is transmitted and reflected by interface 1 and interface 2, the tensile stress $\sigma_{\mathrm{r}2}$ at interface 2 produces reflected stress on the free section of the anchor, and the stresses $\sigma_{\mathrm{r}1}$ and $\sigma_{\mathrm{t}2}$ at interface 2 will be superimposed on the anchorage section of the anchor, therefore, the stress applied by the stress wave on the free section of the anchor is $\sigma_{\mathrm{r}3}$, and the total stress σ_{t} on the anchorage section of the anchor is:

$$\begin{aligned} \sigma_t = \sigma_{r_1} + \sigma_{r_2} &= \frac{1-n_1}{n_1+1}\rho_r c_r k(\frac{Q^{r_3}}{d})^q + \frac{4}{(n_1+1)(n_3+1)}\rho_r c_r \frac{e^{3.95+0.57M_l}}{R} \\ &= \frac{4+(1-n_j)(n_3+1)}{(n_1+1)(n_3+1)}\ \rho_r c_r \frac{e^{3.95+0.57M_l}}{R} \end{aligned} \tag{11}$$

ISSN 2706-655X Vol.5, Issue 12: 106-110, DOI: 10.25236/IJFET.2023.051216

Then, according to the boundary conditions, when z=0

$$\sigma_t = \frac{4+(1-n_j)(n_3+1)}{(n_1+1)(n_3+1)}\rho_r c_r \frac{e^{3.95+0.57M_l}}{R}$$

It can be deduced that

$$\sigma(z) = \begin{cases} \frac{2(1-n_3)}{(n_1+1)(n_3+1)}\rho_r c_r \frac{e^{3.95+0.57M_l}}{R} & (0 \le z < L_1) \\ \frac{4+(1-n_1)(n_3+1)}{(n_1+1)(n_3+1)}\rho_r c_r \frac{e^{3.95+0.57M_l}}{R}\exp\left(-\frac{z^2}{2K}\right) & (L_1 \le z < L_1+L_2) \end{cases} \quad (12)$$

Then the distribution of axial stress on the anchor under combined dynamic-static loading is:

$$\sigma(z) = \begin{cases} \frac{E_b a}{b}\frac{1}{\left(1+e^{-\frac{L_2-x_0}{b}}\right)} + \frac{2(1-n_3)}{(n_1+1)(n_3+1)}\rho_r c_r \frac{e^{3.95+0.57M_l}}{R} & (0 \le z < L_1) \\ \frac{E_b a}{b}\frac{1}{\left(1+e^{-\frac{L_2-x-x_0}{b}}\right)} + \frac{4+(1-n_1)(n_3+1)}{(n_1+1)(n_3+1)}\rho_r c_r \frac{e^{3.95+0.57M_l}}{R}\exp(-\frac{z^2}{2K}) & (L_1 \le z < L_1+L_2) \end{cases} \quad (13)$$

4. Damage forms and criteria of anchored structures under dynamic and static load superposition

When the dynamic load is disturbed, the dynamic load stress wave propagates from the depth of the surrounding rock to the surface of the roadway, and due to the different wave impedance of the free section L1, the anchorage section L2 and the surface of the roadway, the axial stresses superimposed on different locations of the anchors are different. Due to the complex nature of the surrounding rock of the roadway, the differences in the materials of anchor rods and anchoring agents, and the construction errors, the damage form of the anchored bearing structure is different.

For the anchor, when the axial stress on the anchor is greater than the tensile strength of the anchor σ_{b1}, the form of impact failure of the anchor structure is manifested as the bolt breakage. When the axial stress on L2 is greater than the cohesion between the anchoring section and the anchoring agent σ_{b2}, the form of impact failure of the anchoring structure is de-anchoring (the anchor rod falls off from the borehole together with the anchoring agent), and when the axial stress on L2 is greater than the tensile strength of the rock σ_{b3} and is less than the cohesion force between the anchoring section and the anchoring agent, the form of impact failure of the anchoring structure is also manifested as de-anchoring (the anchor rod falls off from the borehole together with the anchoring agent and the surrounding rock).

$$\sigma(z) > \begin{cases} \sigma_{b1}(The\ bolt\ breaks) \\ \sigma_{b2}\ (\text{The bolt is detached from the borehole along with the anchoring agent}) \\ \sigma_{b3} > \sigma_{b2}\left(\begin{array}{c}\text{The bolt is detached from the borehole along with the anchoring agent} \\ \text{and the surrounding rock}\end{array}\right) \end{cases} \quad (14)$$

5. Conclusions

(1) The essence of the stress characteristics of the anchor under the joint action of dynamic load and pre-tensile static load is the dynamic change of the supporting anchor under the action of the dynamic load stress wave, which is not only related to the influencing factors of the dynamic load stress wave, the physical and mechanical properties of the medium, the distance between the disturbance point and the roadway, the size of the disturbance energy, but also related to the anchoring mode of the anchor.

(2) When the axial stress on the anchor is greater than the tensile strength of the anchor σ_{b1}, the form of impact failure of the anchor structure is manifested as the anchor breakage. When the axial stress on L2 is greater than the cohesion between the anchoring section and the anchoring agent σ_{b2}, the form of impact failure of the anchoring structure is de-anchoring (the anchor rod falls off from the borehole together with the anchoring agent), and when the axial stress on L2 is greater than the tensile strength of the rock σ_{b3} and is less than the cohesion force between the anchoring section and the anchoring agent, the form of impact failure of the anchoring structure is also manifested as de-anchoring (the anchor rod falls off from the borehole together with the anchoring agent and the surrounding rock).

ISSN 2706-655X Vol.5, Issue 12: 106-110, DOI: 10.25236/IJFET.2023.051216

References

[1] ZHANG Jianchao, HE Jianqing, JIANG Xin. Force analysis of anchorage section of tension type anchor based on Kelvin solution [J]. Mining and Metallurgical Engineering, 2012, 32(4): 16-19
[2] You Chun'an. Force analysis of full-length bonded anchors[J]. Journal of Rock Mechanics and Engineering, 2000(3): 339-341.
[3] ZHAO Minghua, LIU Sisi, HUANG Lixiong, et al. Numerical simulation calculation of pressure anchor based on energy principle[J]. Journal of Geotechnical Engineering, 2011, 33(4): 529-534.
[4] HUANG Liuyun, ZHANG Peng, ZHANG Shengli. Mechanical analysis of anchored section of CFRP anchors based on Kelvin solution[J]. Journal of Guangxi University (Natural Science Edition), 2013, 38(3): 696-702.
[5] WANG Mingshu, HE Xiuren, ZHENG Yutian. Mechanical modeling of full-length anchors and its application [J]. Metal Mining, 1983(4): 24-29.
[6] YANG Gengshe, HE Tangyong. Pallet effect of full-length anchors[J]. Journal of Rock Mechanics and Engineering, 1991(3): 236-245.
[7] WANG Wenjie, MA Xiongzhong, ZOU Changfu, et al. Tests and problems of FRP anchor support in Jinshandian iron mine[J]. Metal Mining, 2012(10): 1-4+8.